Towards a structural understanding of plant-microbiota interactions using cryo-EM techniques

Liedtke, J.

4

Optimizing cryo-EM Sample Preparation for High-Resolution Imaging of the Ultrastructure of AMF Hyphae

Arbuscular mycorrhizal fungi (AMF) form symbiotic relationships with the majority of vascular plants, acting as mediator in a cross-species trading network of nutrients and resources. Despite their ecological and agricultural importance, key questions remain regarding how AMF regulate the speed and direction of transport within their hyphal networks. In this study, we employed advanced cryo-electron microscopy (cryo-EM) and optimized vitrification techniques to investigate the ultrastructure of AMF hyphae and spores. By improving sample preparation procedures, including the use of newly designed snap-button planchettes, we preserved mature hyphae in a near-native state for high-resolution imaging. This approach revealed consistent cell wall morphology, extensive lipid vesicles with interconnected structures, and clustered organelles along the mature hyphae. These findings provide insight into the cellular organization of AMF and lay a foundation for understanding the structural basis of their trading networks. The methodologies demonstrated here also pave the way for further exploration of AMF-host plant interactions, advancing their potential applications in sustainable agriculture and ecosystem management.

This chapter is based on a manuscript by **Liedtke, J.**, Moravcová, J., Křepelka, P., van Son, M., Nováček, J., Kokkoris, V., Shimizu, T. S., Kiers, T., and Briegel, A.: Optimizing cryoEM sample preparation for high-resolution imaging of the ultrastructure of AMF hyphae, in preparation.

4.1 Introduction

Arbuscular mycorrhizal fungi (AMF) are an ancient group of obligate biotrophic plant symbionts that have been associated with plants for more than 450 million years [13]. AMF are considered key microbionts in the rhizosphere, as they form symbiotic relationships with more than 72% of vascular plant species and even connect various plant species through an extensive hyphal network [134, 135]. This fungal network acts like a biological trading system in which resources and services are exchanged [135]. The fungal partner supplies mineral nutrients, especially phosphorus and nitrogen, and in return receives up to 20% of the plant's photosynthetic products, which is primarily carbon [136].

This mutualistic system enables plants to overcome spatial limitations in nutrient acquisition, and to gain access to resources that would otherwise be too distant to reach. In addition, the fungal network acts as a safety system through which warning signals can be transmitted, allowing plants to respond adaptively to both, biotic and abiotic, stress factors. Furthermore, the hyphal network alters the chemical and physical environment of the surrounding soil through exudates and attracts a diverse community of beneficial microorganisms which, together with the fungal network, form the hyphosphere [136]. These microbial associations enhance the nutrient uptake of the AMF and offer additional protection against competitors and pathogens by forming a biofilm along the hyphal surface. Thus, AMF play a multifaceted role in plant health and ecosystem dynamics that goes beyond nutrient exchange, supporting plant resilience and defence [137].

This complex symbiosis begins when a germinating AMF spore develops an exploratory hypha that branches in response to plant signals, such as root exudates like strigolactones. These signals enable the hypha to move toward the plant by following a gradient of signals in the soil. Upon reaching the root surface, the hypha forms a hyphopodium and awaits the plant's signal to enter its tissue. In response, the plant initiates a process that guides the hypha through its tissue with a penetration apparatus - a membrane that acts as a transcellular tunnel surrounding the penetrating hypha. Once inside, the intercellular hypha spreads along the root axis toward the inner cortical cells. Here, it grows intracellularly and branches into arbuscules. These arbuscules serve as a symbiotic interface for nutrient exchange, with the actual exchange occurring in the perifungal space between the fungal and the periarbuscular membrane.

The arbuscules are temporary structures that can be actively degraded by the plant if nutrient exchange proves insufficient. Additionally, one plant can host multiple AMF strains, including competing strains, simultaneously, allowing it to select the most efficient trading partners. In turn, the AMF can control its cytosolic flux, thus influencing the exchange process, as well. Furthermore, the AMF extends its extracellular hyphal network to seek out other potential trading partners and resources. As part of its life cycle, the AMF also forms new spores, each with strain-specific morphological characteristics. These spores not only facilitate the spread of the fungus to new environments but also provide a basis for AMF taxonomy [138].

The fascinating aspect of this complex symbiosis is how AMF regulate and control resource exchange. In particular, how they transport, divide, and redistribute various goods. Previous studies have attempted to address this question using various microscopic techniques and also in combination with different labelling methods. However, the focus

has often been on the localization and organization of arbuscules in plant tissue, with an emphasis on the arbuscule interface [139, 140]. Only a limited number of studies have investigated the structural composition of the AMF hyphal network and the arrangement of cell organelles within hyphae. Nevertheless, research to date has provided valuable insight into the basic structure of hyphae, demonstrating that AMF contain numerous amounts of mitochondria and multiple nuclei that can be genetically distinct (heterokaryosis). The lumen of aseptate hyphae is largely occupied by elongated vesicles, which often contain lipids. Vesicles of unknown content with varying electron densities were also observed, hypothesized to contain condensed minerals, such as polyphosphates [141]. Other organelles commonly found in fungal cells, such as the endoplasmic reticulum, ribosomes, Golgi apparatus, and microtubules, have also been described in the literature [141]. Observations of cell wall morphology and the plasma membrane indicate a multi-layered structure, similar to that of spore cell walls, although the cell wall morphology of hyphae and spores is clearly different [142, 143]. Furthermore, bacterial and virus-like structures have also been observed within the hyphae [141, 144]. Despite extensive investigation, the structural level at which long-distance transport of goods is regulated remains unclear, and no cellular structure corresponding to a control mechanism has been identified.

As mentioned in previous studies, nearly all microscopic techniques and labelling methods used so far require intensive sample preparation steps. These steps, in one way or another, affect the achievable structural resolution and can compromise sample integrity, obscure finer structural details, and lead to artefacts and misleading assumptions [145]. In order to maintain sample integrity during the sample preparation workflow, a High-pressure freezer (HPF) was used – a procedure in which the sample is rapidly immersed in liquid nitrogen under pressure, preventing formation of crystalline ice and instead preserving the sample in its natural near-native state in vitrified ice [139, 141, 146]. This preservation procedure has been successfully applied to various sample types and has been proven to maintain the sample structure in a near-native state [147]. However, the samples were subsequently treated with freeze-substitution, in which the ice is replaced by a mixture of chemical fixatives, still carrying the disadvantages of chemical fixation [140, 141]. In this study, we are aiming for the development of a sample preparation procedure that preserves the near-native state of the sample throughout the entire sample preparation procedure leading to imaging of the AMF hyphae at high resolution by cryo-electron tomography (cryo-ET). The improvement of sample preparation and the use of cryo-EM will provide further insights into the structural organization of the hyphae, allowing for a more detailed examination of cellular organelles and the cytoskeleton, and potentially reveal a control mechanism for long-distance transport of nutrients.

4.2 Material & Methods

4.2.1 Sample and sample preparation

Rhizophagus irregularis (C2) infected (Ri) T-DNA transformed root organs of *Daucus carota* and *Lycopersicon esculentum* grown on standard MSR medium were provided by the group of Kokkoris & Kiers (Vrije Universiteit Amsterdam/ Netherlands) who received the root organs from Goh [148]. Each plate was divided into two compartments: one with the infected root organ and the other with the fungal compartment covered with cellophane which was

placed on top of the agar. The infected root organ plates were incubated at 25 °C in the dark until use.

In preparation for the vitrification procedure, different approaches were used to harvest the hyphae network and spores from the fungal compartment of the plate. The first approach involved transferring the agar from the hyphal compartment of the plate into a 50 ml falcon tube and liquefying the agar with 10 ml sodium citrate solution (10 mM; pH 6) and vigorous shaking to release the network from the agar [149]. The second, gentler approach involved using the hyphal network that had grown on the cellophane surface layer above the agar. The network was washed off the cellophane with PBS buffer, allowing for a quick transfer to either an electron microscopy (EM) grid or a 3 mm planchette for the subsequent vitrification procedure.

In the later stages of the experiment, germinated spores were used to allow imaging of intact hyphae. First, the spores were separated from the surrounding network by vigorous shaking in 10 mM sodium citrate buffer (pH 6). The remaining network residues were manually removed under a binocular microscope using fine tweezers. To ensure only viable spores were used, dead spores were identified by their distinct colour change after treatment and removed. The viable spores were then placed individually and at a distance on the cellophane surface of an MSR plate (⌀9 cm) and incubated in the dark at 28 °C until germination. For collection, germinated spores were carefully detached from the cellophane surface with a small amount of PBS. Each germinated spore, along with its hyphae, was carefully collected with a 100 µl pipette tip and a small amount of PBS, keeping the sample near the tip opening to prevent adherence to the plastic interior of the pipette tip. The spores were then pooled in a larger drop of PBS on a petri dish. Once all germinated spores and their hyphae were collected, they were transferred to the planchette for high-pressure freezing (HPF) using the pipette tip.

4.2.2 Fluorescence staining of AMF hyphae network and spores

Fluorescent staining was used to localize the hyphal network after HPF and to assess the integrity of the hyphae, distinguishing between intact hyphae with cellular compartments and those that had been damaged during the sample preparation procedure. A combination of fluorescence dyes, mainly Nile Red (NR) and Calcofluor White (CFW) (BactiDrop™, Remel™, Thermo Scientific ™), was used to distinguish and recognize intracellular lipid droplets (NR) and chitin-polysaccharides (CFW). A NR stock solution (10 mg/ml in DMSO; Nile blue A oxazone, Sigma-Aldrich) was diluted 1:100, and 100 µl of this solution pipetted onto the cellophane surface of the fungal compartment of the plate (diameter 9 cm). After 60 min incubation at room temperature (RT) in the dark, excess dye were removed, and 100 µl of 1:46 diluted CFW solution was added. Following an additional 30 min incubation, the plate was washed again with PBS.

In subsequent experiments, additional staining agents such as DAPI (5 µg/ml in PBS; Roche Diagnostics GmBH; Mannheim, DE) and MitoTracker™ Green (1 mM in DMSO; Invitrogen, Oregon, USA) were included in the staining protocol. The DAPI stock solution was diluted 1:5 in a 50% glycerol solution (diluted with MQ), and 200 µl applied on the cellophane surface of the fungal compartment. After an incubation of 15 min in the dark, the excess dye was removed and the plate washed with PBS. Subsequently, 200 µl of

MitoTracker diluted 1:1000 in PBS was added to the fungal compartment of the plate and incubated in the dark for one hour. Subsequently, the excess staining was removed, and the plate washed twice with PBS.

The cellophane with the hyphal network was then transferred to a new petri dish, where the hyphal network was washed off with PBS for further use in the vitrification procedure. The fluorescence staining of the hyphal network was assessed using a fluorescence microscope (DMi8 M; Leica Microsystems GmbH, Austria) prior to freezing.

4.2.3 Vitrification procedure

Vitrification was performed by HPF with a Leica EM ICE (Leica Microsystems GmbH, Austria). The samples were high-pressure frozen either on grids by using a modified waffle method [150] or directly in 3 mm planchettes (Leica Microsystems GmbH, Austria) [151].

AMF waffled grid preparation

For the AMF waffle grid preparation, two approaches were used. The first approach followed the waffle method procedure where the flat side of 3 mm B-planchettes was polished according to the protocol [150]. Additionally, the planchettes were cleaned and coated three times with soy lecithin (1 mM in chloroform). Prior to coating, both sides of the B-planchettes were glow discharged using the H-O UltrAuFoil program (hydrogen 6.4 sccm; oxygen 27.5 sccm; duration 2 min; 40 W; range 5 W) in a plasma cleaner (Solarus II, model 955, Gatan). The grids were also glow-discharged under the same conditions. During the procedure, different grids were tested to improve sample attachment to the grids. The following grid types were used from Quantifoil (Großlöbichau; DE): R2/1-Cu-200; R2/4-Au-200; R1.2/1.3-Au-300 and from Electron microscopy Science (PA; USA): CF100H-Au-50. Later in the experiment, we also tested whether an additional gold layer of 20 nm on the grid would improve sample attachment and recovery after HPF. After preparing the planchettes and grids the waffle sandwich was assembled according to the waffle protocol. The AMF sample was applied to the grid with n-hexadecene before closing the assembly with the flat side the B-planchette. Immediately after, the assembly was HPF and disassembled in liquid nitrogen (LN_2). For further processing, the AMF waffle grid was then clipped into an autogrid.

The second approach for AMF waffle grid preparation were performed using customized snap-button planchettes (unpublished), designed and provided by J. Nováček (CEITEC; Brno; CZ). As in the previous approach, the planchettes were plasma-cleaned and coated three times with soy lecithin on the surface that would face each other during assembly. Additionally, the autogrid rings were also plasma-cleaned and dipped three times in the soy lecithin solution, then air-dried while held with tweezers to prevent damage to the coating from contact with surfaces. Prior to the assembly of the snap-button waffle, plasma-cleaned grids were clipped into the treated autogrid rings. The assembly proceeded as following: first, the stud planchette was placed in a planchette holder resting on tissue, and the clipped grid was positioned on the stud´s dome. The grid was than moistened with a drop of PBS, and AMF samples were applied. Next, the socket planchette was filled with PBS and placed on top of the assembly, allowing excess liquid to be absorbed by the tissue underneath. The assembly was then immediately high-pressure frozen. Following this procedure, the assembly was recovered and disassembled in LN_2. If necessary, the autogrid was detached

from the stud planchette by gently using the tip of an injection needle (⌀0.3 - 0.45 mm, length 13 - 23 mm) to lift it off. The recovered autogrids were stored in autogrid boxes in LN_2 until further use.

AMF planchette preparation

The preparation of AMF planchettes was primarily optimized for AMF spores, which can reach a diameter of up to 150 µm. Prior high-pressure freezing, both A- and B-type planchettes were plasma-cleaned on both side under the same conditions described above. The flat side of each B-planchette was then coated three times with 3 µl of soy lecithin (1 mM in chloroform) per application. To ease differentiation in subsequent procedures, A-planchette side with depths of 100 µm and 200 µm were color-marked. For consistency, only one specific side of each A-planchette was marked and used per session, which comprised up to nine samples.

To apply the samples, the A-planchettes were fist filled with PBS, and the AMF spores were added. The assembly was completed by placing the flat side of a B-planchette on top. Excess liquid was carefully removed by briefly placing the assembly on tissue. The assembled planchettes were immediately after high pressure frozen. Subsequently, the assemblies were recovered and disassembled in LN_2. The color-marked side of each A-planchette was used to identify the side containing the sample. The samples were stored in autogrid boxes in LN_2 until further use.

The AMF planchette preparation were mainly used for the AMF spores, which can be up to 150 µm in diameter. Prior HPF, all planchettes (A and B type) were plasma-cleaned from both sides with the same conditions as described above. Following this treatment, the flat side of B-planchettes were coated 3 times with 3 µl soy lecithin (1 mM in chloroform). The A-planchettes sides with 100 and 200 µm depth, were colour marked for better differentiation in the further procedure. To avoid later confusion, per session of up to 9 samples only one A-planchette side were used and marked. The A-planchettes were filled with PBS and samples applied. Subsequently, the flat side of a B-planchette were used to close the assembly and excess liquid removed by gently placing the assembly briefly on a tissue and immediately after high-pressure frozen. After freezing the assembly were recovered and disassembled in LN_2, whereby the marked side helped to differentiate which side of the A-planchette contained the sample.

4.2.4 Milling of AMF waffle grids & lamella preparation

AMF waffle grids were transferred to an autoloader and inserted into the Arctis Dual-Beam cryo-plasma focus ion beam (PFIB)(Thermo Fisher Scientific™; Oregon; USA) equipped with an integrated fluorescence light microscope module (iFLM) with a quad-band set for imaging samples with simultaneously labelled dyes. Regions of interest were coarsely identified using an electron beam at 25 pA and 2 kV at eucentric height, and fine aligned by fluorescence imaging. The stage was then tilted to -142° for trench milling perpendicular to the ion beam from the back side of the grid. The trenches were milled with a current of 16 nA and had the following dimensions: the side trenches were 1.6 µM wide and 40 µm long; the top trench was 15 µM wide and 10 µm long, and the bottom trench 15 µM wide and 45 µm long. The distance between the trenches for lamella preparation was 15 µM wide and 20 µm long. The trenches were refined by further tilting from 0° to -23° stage tilt

to remove underlying material. The grid was then tilted to 0° and a milling pattern was placed to define the area for the undercut at a tilt angle of -10° and -20° with a nitrogen plasma beam at 4 nA and 30 kV.

After trench preparation, the target area and lamella sites were identified on scanning electron microscopy (SEM) images at eucentric height in comparison with the fluorescence images, and redefined if necessary. A conductive platinum layer was then sputtered onto the grid for 120 seconds at 70 nA and 12 kV Xe plasma to minimize charging effects during lamella preparation. Additionally, a platinum layer with a thickness of approximately 700 nm was deposited over a period of 2 min utilizing a gas injection system (GIS). Each lamella was thinned stepwise at a milling angle of 15° (-23° stage tilt angle) with gradually decreasing beam currents (from 1 nA to 30 pA) until the desired final thickness of 200 nm was reached. The process ended with a polishing step of the lamellae with 10 - 30 pA at 30 kV.

4.2.5 Milling of AMF planchettes & cryo-volume imaging

Prior to the milling procedure, a copper block (20 µm x 10 µm x 10 µm) was prepared from a copper grid and attached to the lift-out needle by re-deposition milling according to the protocol of Schiøtz *et al.* (2024) [152]. Subsequently, an HPF type A planchette and a clipped half-moon grid (Pelco; Kirwan, Australia), loaded in an autogrid, were inserted into a HPF-carrier shuttle (3 mm) with a pretilt of 35°. Subsequently, it was transferred to the cryo-stage of a Helios Hydra V Dual-Beam cryo-PFIB (Thermo Fisher Scientific™) with integrated iFLM (development version) and a cryo-lift-out manipulator. This instrument was used for extraction and transfer of volumes from a bulky HPF samples to a half-moon grid for further processing including lamella preparation.

Prior to imaging, a conductive platinum layer was sputtered onto the planchette using integrated micro-sputter (6 min; 99 nA; xenon plasma). The SEM image of the HPF planchette was acquired (12.5 pA; 2 kV) using MAPS (v.3.25) and aligned with the images acquired with the iFLM (pixel size 110 nm) to identify areas of interest. Subsequently, an approximately 1 µm thick platinum precursor layer was deposited over a period of 1 min using a cryo-deposition with GIS. The protective layer was necessary for subsequent lamella thinning and chunk polishing. The stage was then rotated 180° to proceed with creation of an imaging face. Milling was performed at an angle of 16° (stage tilt 13°) using an ion beam current of 15 nA for rough milling and 4 nA (30 kV) for polishing the imaging face. The trench dimensions were adjusted based on the sample and volume size. Trenches were milled around the volume to be extracted, with overlapping milling patterns. The volume size ranged from 20 µm x 30 µm x 10 µm (L x W x H) to 40 µm x 60 µm x 30 µm (L x W x H).

4.2.6 Serial FIB-SEM Volume Imaging & Volume Lift-Out

The integrity of the sample was verified by volume imaging. Milling was performed at an angle of 16° (tilt angle 13°; ion-beam current 0.6 nA), with SEM imaging at 90° (stage tilt 51°; 25 pA; 1 kV), using AutoSlice&View (version 5; Thermo Fisher Scientific™) and FIBSEM Maestro software (https://github.com/cemcof/FIBSEM_Maestro). Once the integrity of the hyphae was confirmed, the procedure continued with the cryo-lift-out. An additional

platinum layer was applied to the sample surface and the block's leading face for 4 min resulting in a thickness of 1 µm to protect the surface from beam damage during subsequent milling. The stage was configured for perpendicular milling (stage tilt: 17°; rotation: 0°). And trenches around the volume to be extended were milled with a minimum width of 10 µm. The lift-out needle with the attached copper block was moved adjacent to the sample to be extracted. Subsequently, the chunk was attached to the copper block by re-deposition using a single-pass pattern of regular cross-sections at the interface between the copper block and the aligned sample surface [152]. The lift-out was performed at a milling angle of 9° (stage tilt: 6°). The chunk was then transferred to a half-moon grid and the volume aligned by matching its edge to the prepared pin edge, then attached by re-deposition using a single-pass pattern of regular cross-sections (stage tilt: 38°; milling angle: 69°; 300 pA; 30 kV). The lit-out needle was released by milling away the connection between the copper block and the volume surface. After the successful lift-out and attachment to the half-moon grid, the volume and hyphae integrity were rechecked with iFLM, and automated volume imaging was repeated as described above, to fine-tune the positioning for lamella preparation [153]. This step helped to evaluate potential beam damage post-lift-out and created a smooth surface, that minimized milling artefacts during subsequent lamella preparation.

4.2.7 Lamellae Preparation from Volume Samples

The preparation of lamellae from volume samples was performed as described above according to the waffle method protocol [150]. A stage tilt of approx. 10° (milling tilt 13°) was used and the lamellae were thinned with gradually decreasing beam currents, starting from 4 nA, decreasing to 0.3 nA at 2 µm thickness and further to 0.1 nA at 1 µm thickness. At a lamella thickness of 500 nm or less, a beam current of 30 pA was used until the desired final thickness of 200 nm was reached. The process ended with a polishing step of the lamellae at 10 - 30 pA and 30 kV.

4.2.8 cryo-EM data aquisition & processing

Imaging of the prepared lamellae was performed using a 300 kV Titan Krios (Thermo Fisher Scientific™), equipped with a Bioquantum energy filter and a K3 direct electron detector (Gatan). A slit width of 10 eV was used for imaging. The lamellae were aligned perpendicular to the tilt axis of the microscope. Images were acquired at a magnification of 26,000x, corresponding to a pixel size of 3.473 Å. Four tilt series were collected using SerialEM [23] with a dose symmetric tilt-scheme in mode at 2.5° increment. The defocus was set to -6 µm, and the total dose was approximately 80 e-/A^2 with a constant electron dose per tilt image.

4.2.9 cryo-volume SEM data processing

Serial EM images were imported into Fiji and converted into image stacks. The image dimensions were adjusted while maintaining the original width-to-height ratio. Subsequent steps included contrast optimization and alignment using the stack contrast adjustment and template matching plug-ins. Although a stack suitable for 3D reconstruction was generated, a final volume rendering was not performed due to the absence of a consistent structural reference across slices, which impeded reliable spatial correlation.

4.3 Results

4.3.1 Sampling techniques for AMF hyphal network and spores

The AMF samples were taken from the plates using different sampling techniques and transferred to either an EM grid (Fig. 4.1) or a planchette (Fig. 4.2), optimizing the process to ensure that the integrity of the samples was largely maintained. The use of the AMF hyphal network growing on the cellophane surface of the AMF plate resulted in a higher number of intact hyphae after high pressure freezing compared to other techniques. In this approach, the cellophane with the hyphal network was transferred to a new petri dish. Here, the network was gently washed off from the cellophane surface with PBS. This method enabled more efficient sampling and increased the likelihood that some of the hyphae remain intact for subsequent analysis. In contrast, the commonly used sodium citrate buffer method, in which the hyphal network is released by liquefying the agar, leads to loss of the cell content and predominantly empty hyphae. However, the sodium citrate buffer method was still the most effective way for extracting spores from the medium with minimal hyphal residue. The subsequent manual sorting of larger or dead spores, which were identifiable by a change in colour, also improved vitrification outcome.

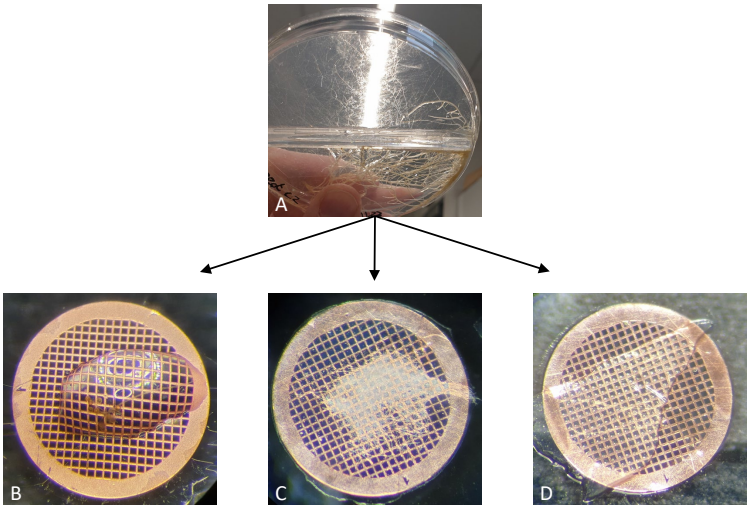

Figure 4.1: Sampling of AMF for cryo-EM sample preparation. The AMF plate consisted of two compartments separated by a membrane: one side contained the AMF with its host roots, while the other contained the hyphal network and spores. In the hyphal compartment, the medium was overlaid with cellophane to prevent desiccation, with the hyphal network and spore growing both within the medium and on top of the cellophane. (A) AMF plate showing the two compartments: AMF with host roots and hyphal compartment. (B) Spores with residues of hyphal network, released using the sodium citrate buffer method. (C) Hyphal network extracted from the medium by vigorous shaking the medium in sodium citrate buffer. (D) Cellophane section with branched hyphae. All samples were transferred either to a 3 mm planchette or to a 3 mm copper grid for further sample processing by high-pressure freezing.

Overall, the cellophane-surface sampling technique proved to be the most effective method for maintaining the integrity of the AMF hyphae and providing a reliable method for cryo-EM sample preparation and analysis.

In the later stages of the experiment, young germinated spores with their fragile germ tubes (young hyphae) were also used. The advantage of this technique is that the hyphae do not need to be cut, so their cell content remain intact. Handling these samples was challenging, as the germ tubes are fragile and can break during harvesting and transfer to the high pressure freezing assembly. To address this issue, the spores with their fragile germ tube were first detached from the cellophane surface with a small amount of PBS. Subsequently, a 100 µl pipette tip was partially filled with PBS and used to transfer the spores and germ tubes. To prevent loss of the sample by adhering to the tip's plastic surface, the filled pipette was depressed to keep a small drop of PBS on the tip, which was used to pick up the sample and transfer it to the high pressure freezing assembly. For efficiency and to increase the amount of sample material on the planchette, spores with their germ tubes were first collected in a larger PBS droplet and then transferred together using the described procedure (Fig. 4.2).

We also attempted to target specific areas of the hyphal network, particularly where hyphae branched, by cutting small pieces of cellophane containing these areas and directly placing them on a waffle grid for high pressure freezing (Fig. 4.1D). Although this approach was time-consuming, it allowed precise selection of specific hyphal regions. Notably, the cellophane proved suitable for PFIB milling, enabling access to the sample. However, this method introduced an additional layer of thickness, which increased the time required for subsequent milling. Additionally, prolonged handling during transfer onto the grid occasionally compromised hyphal integrity. To minimize leakage from the hyphae, one side was initially separated from the network, allowing a plug to form at the cut edges before detaching the other side.

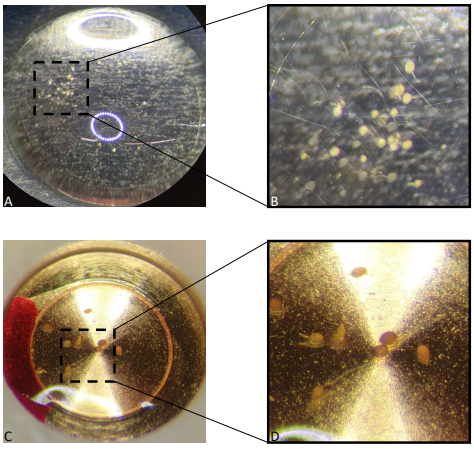

Figure 4.2: Germinated spores with germ tubes. (A, B) Germinated spores with intact germ tubes collected in a small PBS droplet. (C, D) The collected spores were transferred into a planchette to increase sample material, with spores and spores remaining intact.

4.3.2 Improved detectability through fluorescence staining

The use of fluorescent dyes to stain specific cell components significantly improved the detection of intact AMF hyphae suitable for lift-out and lamella preparation. At the beginning of screening of vitrified samples, we found that the detection of hyphae and spores after high-pressure freezing was challenging due to the formation of an almost uniform layer on the sample surface (Fig. 4.3A). In some cases, individual hyphal membrane structures were visible on the ice surface (Fig. 4.3B). However, these structures often exhibit low sample integrity during milling, making them unsuitable for lift-out and lamella preparation, as they would fragment during further processing. Therefore, the sample surface had to be milled blind, which was time-consuming and often led to suboptimal results.

The use of fluorescent dyes significantly enhanced the detectability of the sample material. Additionally, the targeted application of specific fluorescent dyes enabled selective milling of certain cellular components (Fig. 4.3C & D). The combination of these dyes further improved the process, allowing for differentiation between intact and non-intact hyphae prior to milling (Fig. 4.3E & F). This approach increased the likelihood of identifying intact hyphal regions suitable for further processing.

4.3.3 Vitrification methods for AMF samples

The modification of the waffle method using a newly designed snap-button planchette (J. Nováček; CEITEC Masaryk University; Brno; CZ ;unpublished) enabled the vitrification of samples with larger volumes, making it suitable for cryo-EM imaging of AMF hyphae (Fig. 4.4). When applying the waffle method, we encountered several challenges partly due to the characteristics of the sample. AMF spores, for instance, display significant size variability and age-dependent differences in wall thickness, both of which can affect the vitrification process. Additionally, AMF hyphae showed a low affinity to metallic surfaces and even show repulsive behaviour, complicating their application to copper grids despite additional coating with carbon or gold. This repulsion sometimes led to the loss of sample as the material adhered to the edges of the grids or other surfaces.

To overcome these challenges, custom-designed snap-button planchettes were used in subsequent experiments (Fig. 4.4). These planchettes allowed the use of clipped grids, with the clip ring providing an additional 100 µm of space for the sample (Fig. 4.4D & F). This extra space enabled the application of a small drop of buffer or cryoprotectant onto the grid, forming a dome that facilitated the transfer and positioning of AMF hyphae onto the grid. The snap-button planchettes reduced the assembly time needed and increased the recovery rate of intact grids following high-pressure freezing. By pre-clipping the grid, it minimized the risk of sample loss during post-freezing clipping. Moreover, the snap-button method was also suitable for young and small spores, though direct high pressure freezing of AMF spores in planchettes was more suitable for handling a range of spore sizes and was similarly advantageous for high-pressure freezing of germinated spores (Fig. 4.2).

After high-pressure freezing the autogrid (clipped grid) was loaded into a PFIB, the area of interest was identified using fluorescence microscopy and compared with SEM imaging (Fig. 4.5). The milling pattern was then applied using the waffle method, and the milling process was initiated. During lamella preparation, the milling process had to

be monitored regularly to ensure that the final lamella contained hyphae and was not over-milled (Fig. 4.5B & C). This was particularly important, as fluorescence and SEM microscopy could only provide a rough estimate of the Z-height of the area of interest. As shown in figure Fig. 4.5B, when it became evident during rough milling that the area of interest (hyphae) had been missed or milled away, the milling position was adjusted and rough milling was repeated. Such adjustments were more manageable during the rough milling stage compared to the fine milling stage, where the risk of damaging or losing the newly prepared lamella increased. Additionally, a change in the gas used for the plasma-focus ion beam was necessary, as the nitrogen-based beam proved to be too rough for fine milling, causing curtaining and even fracturing of the lamella. Therefore, oxygen plasma was used for the fine milling steps, as it minimized the curtaining effect and allowed the successful preparation of a lamella from hyphae with a thickness of approximately 200 nm. Overall, the use of custom-designed snap-button planchettes significantly improved the efficiency and reliability of vitrification for AMF samples.

4.3.4 Challenges during milling and serial-SEM imaging

As mentioned above, different sample extraction procedures let to various complications and artefacts, which often only became evident during PFIB-SEM or even later during cryo-EM analysis. One of the most common issues encountered during PFIB milling was the presence of empty hyphae, which had lost their contents during sample extraction (Fig. 4.6). The use of sodium citrate buffer in the extraction process resulted in loss of cellular content, sometimes causing cavities within the hyphae (figure 4.6B & D). This negatively affected the high-pressure freezing process and led to suboptimal vitrification of the AMF sample.

To address these challenges and improve the preservation of cellular content, we decided to use hyphae material obtained from the cellophane surface. This method, being gentler, allowed for significantly faster processing from hyphae extraction to high-pressure freezing, leading to better sample preservation. While it also contributed to improved vitrification, the primary benefit was in maintaining the sample's integrity. Additionally, the choice of cryoprotectant used during HPF played a crucial role in maintaining sample integrity and reducing PFIB milling time.

Hexadecene, a widely used cryoprotectant, caused the hyphae to react repulsively, making it difficult to apply the sample onto the grid or planchettes, thus increasing the time required to prepare the sample for high-pressure freezing. This prolonged preparation time further complicated the process of obtaining sample with high cell integrity.

Moreover, vitrified hexadecene was found to be a hard material, which prolonged milling times. Another disadvantage of using hexadecene was the frequent occurrence of cracks and fractures in the vitrified sample during milling (Fig. 4.6C & D). These issues were likely due to the increased beam exposure time required by the higher material hardness of hexadecene.

An alternative cryoprotectant, PBS, proved to be more suitable for AMF samples. Hyphae reacted more favourable to PBS, and it also facilitated faster milling. Although cracks and fractures still occurred during milling in samples vitrified with PBS, their frequency was lower compared to samples vitrified with hexadecene.

Apart from the challenges mentioned above, the variability of the hyphae also posed a challenge during milling and serial imaging. Hyphae can contain various types of minerals transported through the hyphal network, which can exhibit different charging effects, leading to artefacts during serial imaging in the slice & view procedure. By optimizing extraction, using PBS as a cryoprotectant and applying oxygen-based plasma for fine milling, challenges such as low sample integrity and artefacts were mitigated, improving serial-SEM imaging and lamella preparation.

In addition to the hyphae, spores of different sizes and maturities were also vitrified. During the course of the experiments, it became apparent that the vitrification of older, more mature spores was often inconsistent and unreliable. Furthermore, mature spores exhibited considerable hardness during milling, requiring a higher beam intensity, which led to beam-induced damage to the more sensitive spore contents (Fig. 4.7A&B). In contrast, small, young spores allowed for the successful production of lamellae, although the spore cell wall remained a challenging material to mill, often requiring several hours or even days to fully mill through (Fig. 4.7C&D). Initial lamella preparations were promising but due to the different material properties of the spore cell wall and its contents, the lamellae frequently disintegrated and were lost during the fine milling procedure. As a result, the focus of the experiments shifted towards lamella preparation and subsequent cryo-EM data collection of mature hyphae.

4.3.5 Challenges in AMF hyphal ultrastructure visualization

Cryogenic sample preparation enabled detailed insights into the hyphae and the spatial organization of their cell content, primarily consisting of lipid vesicles (Fig. 4.8). Other cell organelles, as well as the various layers of the cell wall and plasma membrane, were visualized in a near-native state. Further processing of the vitrified AMF hyphae using PFIB-SEM and the slice & view approach enabled serial imaging and provided a dataset suitable for 3D reconstruction (Fig. 4.8). After confirming the integrity of the hypha through serial-PFIB-SEM, lamellae were produced from the sample volume.

Due to the large sample volume, another challenge arose: the increased relocation of ice and milling residues, which preferentially deposited on charged surfaces such as the surrounding area of the milled lamella or directly on the lamella surface (Fig. 4.9). This contamination led to longer milling times and often resulted in the loss of lamellae. The risk of ice crystal contamination increased during the transfer from PFIB-SEM to cryo-EM, leading to a continued reduction in lamellae quality or in many cases, additional lamellae loss. In particular, loading and unloading of the samples into different cryogenic devices was the most critical point where most contamination and lamella loss occurred. Only a few lamellae were suitable for cryo-EM imaging. Despite these challenges, preliminary cryo-EM images obtained from hyphae provided early insight into their ultrastructure at near native state.

As shown in figure 4.9, a network of vesicle-like structures and bundles of filaments were imaged. Although lamellae preparation and contamination presented challenges, the initial cryo-EM imaging revealed high-resolution structural features of mature AMF hyphae in a near-native state.

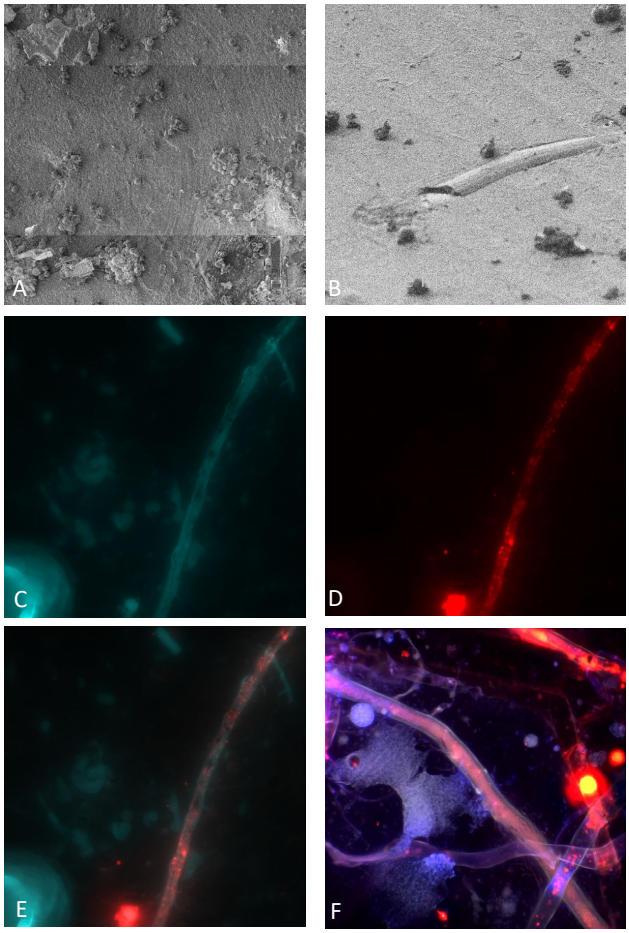

Figure 4.3: Fluorescence labelling of AMF hyphae. Fluorescence labelling facilitated the identification and targeted milling of AMF hyphae within the ice layer. (A) Nearly uniform ice layer on the grid surface after high pressure freezing, which made the detection of AMF hyphae for PFIB milling difficult. (B) AMF hyphae membrane on the surface of the ice layer on grid. (C) AMF hyphae stained with CFW, which labels chitin and cellulose. (D) AMF hyphae stained with NR, which labels membrane lipids and lipid vesicles. (E) Combined CFW and NR staining for identification of intact hyphae areas. (F) Multi-dye fluorescence labelling (DAPI; Mitotracker; CFW; NR) used to target specific cellular compartments, including mitochondria (Mitotracker) and nuclei (DAPI).

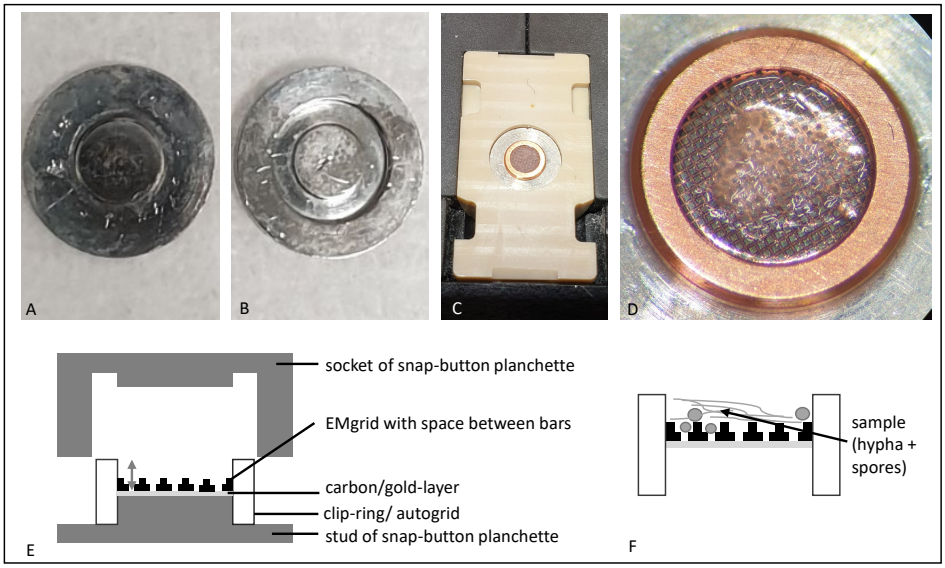

Figure 4.4: Snap-button planchette for high-pressure freezing of larger volume samples. (A) Stud and (B) socket of snap-button planchette (6 mm). (C) Positioning of clipped grid and assembly of snap-button planchette. (D) AMF hyphal network applied to the centre of clipped grid within the assembly, after moistening with a drop of PBS to improve sample adherence and positioning. (E) Schematic representation of snap-button planchette assembly, with the grey arrow indicating sample space. (F) Schematic representation of the sample space on a clipped grid.

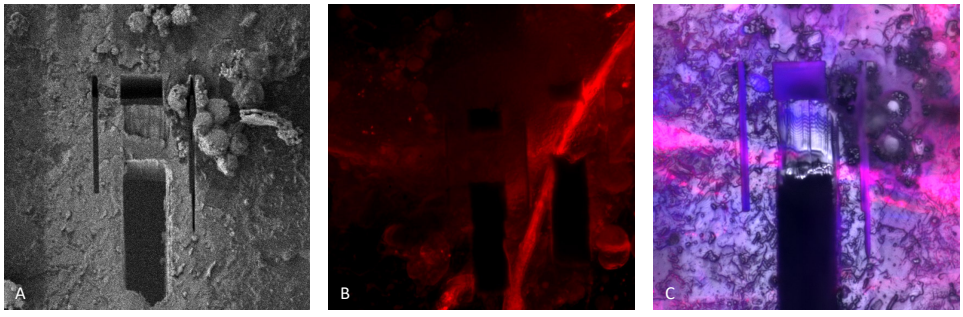

Figure 4.5: Lamella preparation of AMF hyphae sample. (A) Rough milling of trenches using artefacts as orientation points on the nearly uniform ice layer. (B) Placement of milling pattern for rough milling, aligned with fluorescence microscopy, and adjustment of pattern positioning if the area of interest was missed. (C) Alignment of SEM and fluorescence imaging of final lamella, with hyphae material positioned on the lower edge. Despite imprecise Z-height positioning leading to missed half of hyphae material during fine milling, a fine lamella (~200 nm thick) was successfully milled and transferred for cryo-EM imaging.

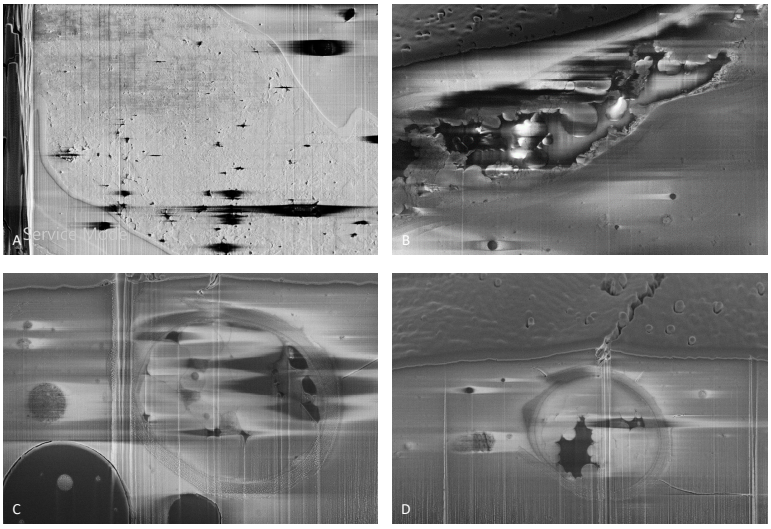

Figure 4.6: SEM images of AMF hyphae during milling using PFIB-SEM, showing various artefacts from sample treatment and HPF procedure. (A) Lateral view of a hyphae that has lost its cellular content, with only the cell wall and collapsed plasma membrane remaining. (B) Lateral view of a partially filled hyphae, showing large gaps due to the loss of cellular content. (C, D) Front view of partially filled hypha, showing artefacts such as cracks and holes in the surrounding ice, which challenged further processing.

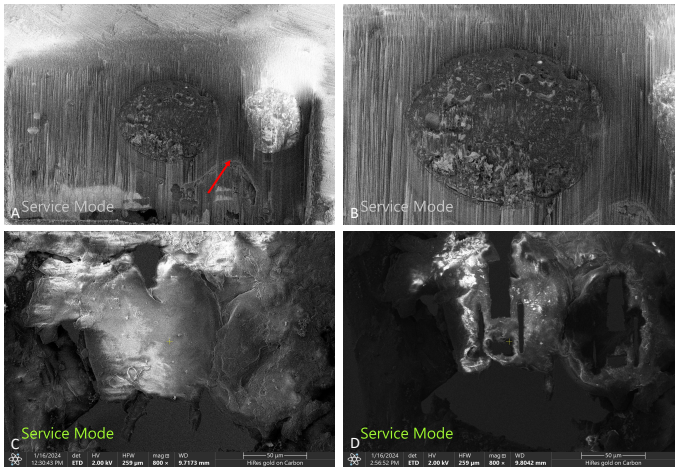

Figure 4.7: SEM images of AMF spores during rough milling, acquired using PFIB-SEM in preparation for lift-out and lamella milling. (A; B) Milling of a mature spore required the use of higher voltage due to the thick, multilayered spore cell wall, resulting in milling artefacts and beam-induced damage to the spore contents. (C) Small spores vitrified on a grid used for (D) lamella preparation. The red arrow points to a hyphal connection between the spore and the hypha.

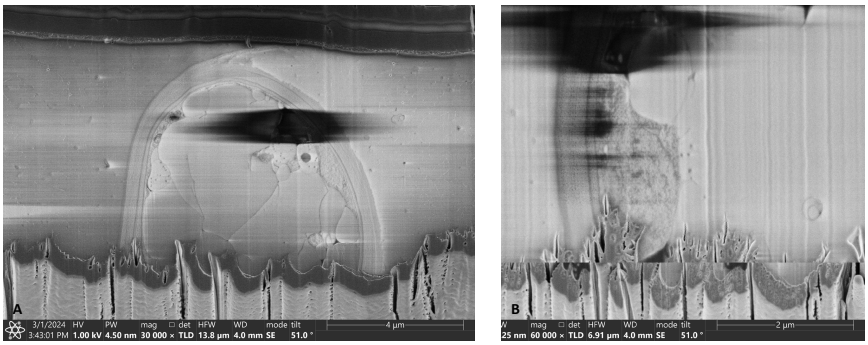

Figure 4.8: SEM images of a nearly intact hyphae obtained using autoslice & view approach at a PFIB-SEM. (A) Front view of a hyphae with nearly intact cellular content. (B) Detailed view of the cell wall layers and cell organelles. Scale bar: (A) 4 µm; (B) 2 µm.

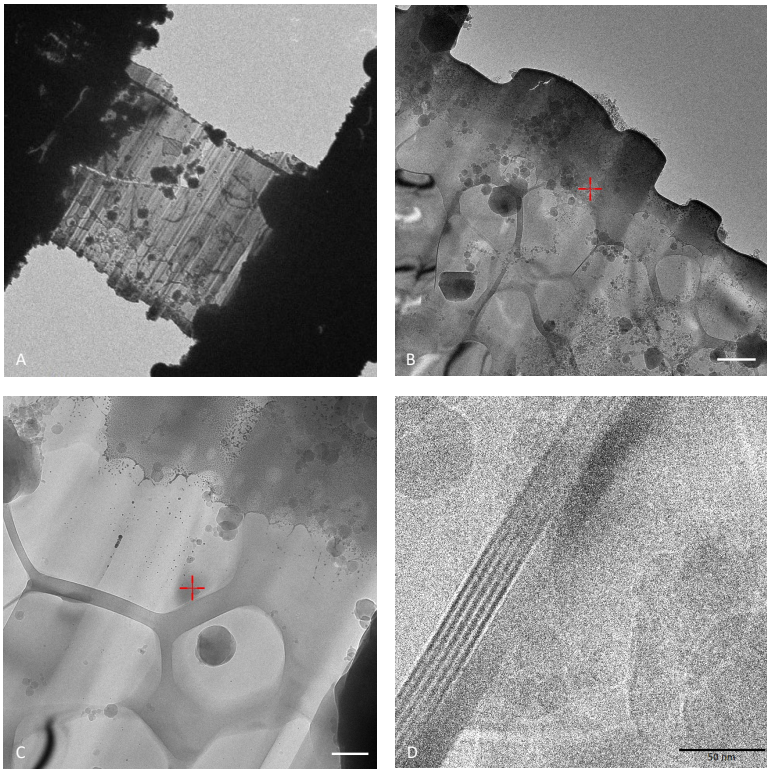

Figure 4.9: Lamella of AMF hyphae and initial cryo-EM images. (A) Lamella containing hyphae, surrounded by ice crystal contamination. (B; C) Detailed view of hyphal content, showing a fine network between vesicles. (D) Cryo-EM image of a filament bundle of AMF hyphae, which could not be further classified due to their unclear positioning. Scale bar: (B) 500 nm; (C) 200 nm; (D) 50 nm.

4.4 Discussion

We know that high-resolution insight into 3D structures is a powerful tool to gain a detailed understanding of cellular components and their interactions. Cryopreservation preserves the cellular ultrastructure in near-native state, while advanced cryo-ET techniques enable high-resolution 3D visualization that allows the spatial distribution of cellular components to be studied in unprecedented detail. In this study, we applied and successfully modified the cryo-EM sample preparation procedure making it suitable for AMF samples, including hyphal network and spores, enabling high-resolution imaging of their ultrastructure. Improvements in sample handling allowed better preservation of the cellular content of mature hyphae while high-pressure freezing and to continue further sample processing in cryo-stage preserved the ultrastructure of the AMF samples. This breakthrough enabled, for the first time, the visualization of mature AMF hyphae and the investigation of distribution patterns of cell organelles, their interaction with the plasma membrane, and potential contributions to bidirectional transport of goods.

In the initial stages, the waffle-method was used for high-pressure freezing [150]. This method involves placing the sample on a grid sandwiched between the flat sides of two B-planchettes. While this approach is described in the literature as effective for samples up to 25 µm (width) x 50 µm (depth) and a length up to 100 µm [150], it presented several difficulties when applied to AMF samples. One major limitation was the restricted sample thickness, determined by the grid bar depth, typically limited to around 50 µm. This depth could be extended by 50 µm using a metal spacer (3 mm), but this introduced additional challenges. During the HPF process, the assembly of grid, spacer, and sample frequently slipped, leading to misalignment of the sample relative to the grid centre. If the sample was positioned too far-off centre, it became difficult and even impossible to process further in the PFIB-SEM or cryo-EM due to the physical limitations of ion beam alignment on the sample. Furthermore, the samples showed a tendency to be repulsive to metal surfaces, making it challenging to apply and to position the sample at the centre of the grid.

After HPF, recovering intact grids became another significant issue. The disassembly process often damaged or deformed the grids, leading to a low recovery rate of usable sample-grids (HPF grid with sample material). The subsequent required clipping of sample-grids for the further sample processing introduced additional complications. This extra handling step increased the risk of ice crystal contamination and frequently caused detachment and complete loss of sample material during clipping.

Given these challenges, the original waffle-method proved unsuitable for preparing AMF samples for vitrification and subsequent lamella preparation procedure.

To overcome the limitations, we modified the existing waffle method to make it more suitable for AMF samples and other larger-volume samples (50 – 150 µm thickness). One key adjustment was the use of pre-clipped grids (autogrids) in the HPF carrier-sample assembly. This change streamlined the process, reduced the risk of sample loss and minimized the risk of ice crystal contamination. The clip ring height also provided approximately 100 µm of extra sample space, enabling better accommodation of thicker samples (up to 150 µm). Additionally, the clip ring protected the sample-grids (HPF grids with sample material) during disassembly, contributing to a higher recovery rate of intact sample-grids. While traditional planchettes with sample spaces of 100 to 300 µm (per side) were typically used

for larger volume samples (>10 µm), this often led to excess cryoprotectant surrounding the sample [154]. This in turn, required more extensive milling during the lift-out procedure and lamella preparation. To minimize this, a new planchette design, termed snap-button planchettes, was introduced. This redesign facilitated smoother disassembly, increasing the likelihood of obtaining intact sample grids while ensuring proper sample positioning during high pressure freezing. The reduced surrounding volume also minimized the cryoprotectant usage and subsequent milling efforts.

Although the modifications developed in this study significantly improved the vitrification quality of AMF samples and greatly increased the recovery rate of intact sample grids after high-pressure freezing, challenges remain. A particular low success rate of milling thin lamellae and even fewer successful cryo-EM imaging sessions due to ice crystal contamination still hinder consistent outcomes. Addressing these limitations, a potential solution could involve integrating an ice crystal and milling residue trapping system, similar to the cold finger anticontaminators used in transmission-electron microscopy (TEM). This system could be adapted to not only provide a cold surface to attract particles but also incorporated a charged layer specifically designed to trap ice and milling residues. A charging layer could be created through a surface charging step, where a targeted region of the trap is charged by milling a small surface, creating a charged region that efficiently traps contaminants.

The trap could ideally be applied throughout the entire milling process, with the most significant reduction in contamination risk likely occurring during the fine milling step. At a minimum, it could be applied also only during fine milling of the lamellae. However, further testing and development are needed to validate this approach.

Another important avenue for improvement lies in optimizing fluorescence microscopy at cryogenic temperatures. Testing a range of fluorescence dyes to identify those that are suitable for cryogenic conditions, with low photobleaching during milling and imaging, is crucial. The use of cryo-compatible dyes, especially those that can specifically target cellular organelles such as ER-Tracker or BODIPY-brefeldin A — successfully applied in other fungal system [155] — would significantly enhance the ability to identify and localize organelles within AMF hyphae. This would not only aid in organelle classification but also facilitate deeper insights into their roles in nutrient transport, storage, and the underlying regulatory mechanisms.

Using the advanced vitrification method for AMF samples described above, we were able to image mature hyphae in unprecedented detail, revealing their ultrastructure in a near-native state. The cell wall morphology was consistent across mature hyphae, regardless of their diameter. As previously reported in the literature, hyphae were primarily filled with lipid vesicles. However, in contrast to other studies that mainly investigated germ tubes and young hyphae, the lipid vesicles in the mature hyphae often appeared large and interconnected, with indistinct boundaries. Cell organelles were distributed along the hyphae but frequently clustered together. Some were positioned on the plasma membrane, while others were distributed within the cytoplasm. Initial cryo-EM images suggested a network-like structure among the vesicles, though further investigations are needed to confirm these findings. Notably, no septum or additional layer was identified that could explain the organization of the bidirectional transport system within the hyphae.

While these biological insights shed light on the structural complexity of AMF hyphae, the technical challenges in preserving these delicate features required significant refinement of the high-pressure freezing process.

Looking ahead, as advancements in lamella preparation for large-volume samples continue to evolve, the success rate for imaging such samples at high resolution is expected to improve rapidly. The methodologies developed in this study, including the optimized sample preparation of mature AMF hyphae and the design of snap-button planchettes, are well-positioned to play a pivotal role in advancing research in this field. These methods pave the way for high-resolution cryo-ET data collection, offering unprecedented opportunities to investigate AMF ultrastructure in a near-native state and to address fundamental questions in AMF biology with greater clarity and precision.

Acknowledgements

J.L. was supported by the OCENW.GROOT.2019.063 and Building Blocks of Life 737.016.00 grants from the Netherlands Organization for Scientific Research (NWO), both awarded to A.B. This work benefited from access to the Electron Microscopy facility in Brno, Czech Republic, an Instruct-ERIC centre. Financial support was provided by Instruct-ERIC (PID: 27640) as well as through the Instruct-ERIC Internship Call (APPID: 3188). We also gratefully acknowledge the CF CEITEC/Brno – Cryo-electron Microscopy and Tomography facility of CIISB, Instruct-CZ Centre, supported by MEYS CR (LM2023042) and the European Regional Development Fund – Project „Innovation of Czech Infrastructure for Integrative Structural Biology“ (No. CZ.02.01.01/00/23_015/0008175).

Author Contributions

J.L. developed the sample preparation and cryo workflow, designed and coordinated the study, performed most experiments including sample preparation, vitrification, fluorescence imaging, and initial cryo-PFIB/SEM sessions, and wrote the manuscript. J.M. and P.K. provided training and technical support at CEITEC, jointly operated the cryo-PFIB/SEM system with J.L., and carried out lamella preparation, lift-out procedures, and cryo-EM data acquisition. They also contributed to the PFIB/SEM Methods section. M.v.S. prepared the AMF(C2) infected (Ri) T-DNA transformed root organ plates, provided additional sample material, and supported the preparation of germinated spores. J.N. designed the snap-button planchette and provided technical advice. V.K. provided scientific input. T.S.S. and T.K. supervised the Amsterdam component and enabled the collaboration. A.B. supervised the project and provided feedback on the manuscript.